SANDIA REPORT
SAND2022-13801
Printed October 2021

Sandia National Laboratories

Nanoparticle Mediated Delivery of Therapeutic mRNA for Protection Against Lung Damage

Steven Branda (8623), Richard Mosesso (8623), Anupama Sinha (8621), Christine Thatcher (8621), Nicole Collette (LLNL), Ashlee Phillips (LLNL), Tanya Tanner (LLNL)

Prepared by
Sandia National Laboratories
Albuquerque, New Mexico
87185 and Livermore,
California 94550

Issued by Sandia National Laboratories, operated for the United States Department of Energy by National Technology & Engineering Solutions of Sandia, LLC.

Available to DOE and DOE contractors from
U.S. Department of Energy
Office of Scientific and Technical Information
P.O. Box 62
Oak Ridge, TN 37831

Telephone: (865) 576-8401
Facsimile: (865) 576-5728
E-Mail: reports@osti.gov
Online ordering: http://www.osti.gov/scitech

Available to the public from
U.S. Department of Commerce
National Technical Information Service
5301 Shawnee Rd
Alexandria, VA 22312

Telephone: (800) 553-6847
Facsimile: (703) 605-6900
E-Mail: orders@ntis.gov
Online order: https://classic.ntis.gov/help/order-methods/

ABSTRACT

Medical countermeasures (MCMs) based on messenger ribonucleic acid (mRNA) are promising due to their programmability, targeting precision and specificity, predictable physicochemical properties, and amenability to scalable manufacture. However, safe and effective delivery vehicles are needed, especially for targeting the lung. We developed a generalized approach to nanoparticle-mediated mRNA delivery to lung, and used it to evaluate candidate therapies. In initial studies, reporter mRNA was delivered using lipid-coated mesoporous silica nanoparticles (LC-MSNs) and lipid nanoparticles (LNPs), the latter with greater consistency. Then, mRNA encoding known protein therapies were delivered using LNPs. These formulations showed some toxicity in mice with lung damage, but those with IL-1RA, sACE2-Ig, and ANGPT1 mRNA were modestly therapeutic on balance. Our work advances the state of the art for mRNA delivery to lung, and provides a foundation for evaluating and characterizing mRNA-based lung therapies, including three that appear to be exceptionally promising.

CONTENTS

LIST OF FIGURES

LIST OF TABLES

ACRONYMS AND TERMS

Acronym/Term	Definition
MCM	medical countermeasure
NA	nucleic acid(s)
RNA	ribonucleic acid(s)
mRNA	messenger ribonucleic acid(s)
DNA	deoxyribonucleic acid(s)
WMD	weapon of mass destruction
DoD	United States Department of Defense
NIH	National Institutes of Health
SNL	Sandia National Laboratories
NP	nanoparticle
LC-MSN	lipid-coated mesoporous silica nanoparticle
LC-MSN (hex)	LC-MSN(s) in hexagonal pore structural configuration
LC-MSN (stellate)	LC-MSN(s) in stellate structural configuration
LNP	lipid nanoparticle
mol%	molar fraction
hApoE3	human apolipoprotein E3
hApoE4	human apolipoprotein E4
fLuc	firefly luciferase
IVIS	*in vivo* imaging system
siRNA	small interfering ribonucleic acid(s)
CRISPR	clustered regularly interspaced short palindromic repeats
RNP	ribonucleoprotein
mo	month(s)
d	day(s)
h	hour(s)
min	minute(s)
sec	second(s)
OPA	oropharyngeal aspiration
IV	intravenous
IP	intraperitoneal
PBS	phosphate buffered saline
LOD	limit of detection
AU	arbitrary units

Acronym/Term	Definition
Ab	antibody
FDA	Food and Drug Administration
IVT	*in vitro* transcription
HRP	horse radish peroxidase
ARDS	acute respiratory distress syndrome
LPS	lipopolysaccharide
NKT	natural killer T
αGalCer	α-galactosylceremide
NHP	non-human primate

1. INTRODUCTION

Nucleic acid (NA) based medical countermeasures (MCMs) hold tremendous promise due to their programmability, targeting precision and specificity, predictable physicochemical properties, and amenability to scalable manufacture [1]. Those based on messenger ribonucleic acid (mRNA) could prove especially useful because they combine *in situ* amplification (each mRNA molecule directs production of multiple copies of its cognate protein, such that small amounts of effectively delivered mRNA can have large impact), transience (mRNA lifetime determines duration of protein production, and it can be manipulated), and low risk of interference with the host genome [whereas deoxyribonucleic acid (DNA) can generate mutations through recombination, for instance] [2]. However, translation of mRNA-based MCMs to clinical use has been stymied by lack of safe and effective delivery vehicles, especially those mediating delivery to the lung [3,4,5]. This bottleneck has become increasingly problematic for federal agencies tasked with countering weapons of mass destruction (WMDs) [*e.g.*, Department of Defense (DoD)], many of which primarily target, or cause severe collatoral damage to, the lung; and those tasked with maintaing public health [*e.g.*, National Institutes of Health (NIH)], which would greatly benefit from MCMs that promote lung resiliency to stress, damage, and disease. Development of an efficient and safe means of delivering mRNA-based MCMs to lung would significantly advance medicine and improve our ability to maintain the health of our nation's military and civilian populations.

Sandia National Laboratories (SNL) previously developed lipid-coated mesoporous silica nanoparticles (LC-MSNs) as a modular and biocompatible platform for targeted *in vivo* delivery of diverse cargo, including small-molecule compounds, peptides, proteins, DNA plasmids, and small interfering RNA (siRNA) [6]. In testing whether LC-MSNs can be outfitted for delivery of a much larger and more complex cargo [the clustered regularly interspaced short palindromic repeats (CRISPR)/Cas9 ribonucleoprotein (RNP) complex] to lung, we made an unexpected discovery: A control cargo – mRNA encoding Cre recombinase – was delivered to lung with exceedingly high efficiency in all four animals tested **(Figure 1, panel 4)**, with no off-target delivery detected (**panel 10**). In contrast, commercially-available transfection reagents were found to mediate little to no detectable delivery of Cre mRNA to lung (**panels 5 and 6**, respectively), with similar degrees of delivery observed in off-target tissues (**panels 11 and 12**). These were very promising findings, as they suggested that LC-MSNs could serve as effective NP-based vehicles for delivery of mRNA to lung. Accordingly, we proposed to carry out studies designed to definitively confirm these findings, use them to inform development of a generalized approach to NP-mediated delivery of mRNA to lung, and demonstrate the utility of this approach in evaluating candidate mRNA-based MCMs as lung therapies. In brief, the Specific Aims of our project were as follows:

- Aim 1: Confirm that NPs effectively deliver reporter-encoding mRNA to lung.
    - Initially, we used a more specific expression of Aim 1: "Confirm that LC-MSNs effectively deliver Cre mRNA to lung". However, in light of our findings and the project's evolution, we revised the language to reflect a more general approach. Similar revisions were made to the other Aims as well.
    - This Aim also incorporates optimization and characterization of NP-mediated delivery of reporter-encoding mRNA to lung (initially called Aim 2), as these activities were carried out simultaneously with confirmation of delivery.
- Aim 2: Determine whether NPs can effectively deliver candidate therapeutic mRNA to lung.
    - Initially, this was called Aim 4, and preceded by an Aim 3 that read: "Determine whether NPs can effectively deliver other mRNA to lung". As the project progressed, it was recognized that this Aim would be accomplished through study of the candidate therapeutic mRNA, and so the redundancy was removed.

This report summarizes our efforts to address these Specific Aims, the results that they yielded, the implications of our results, and our perspective on potentially productive future directions.

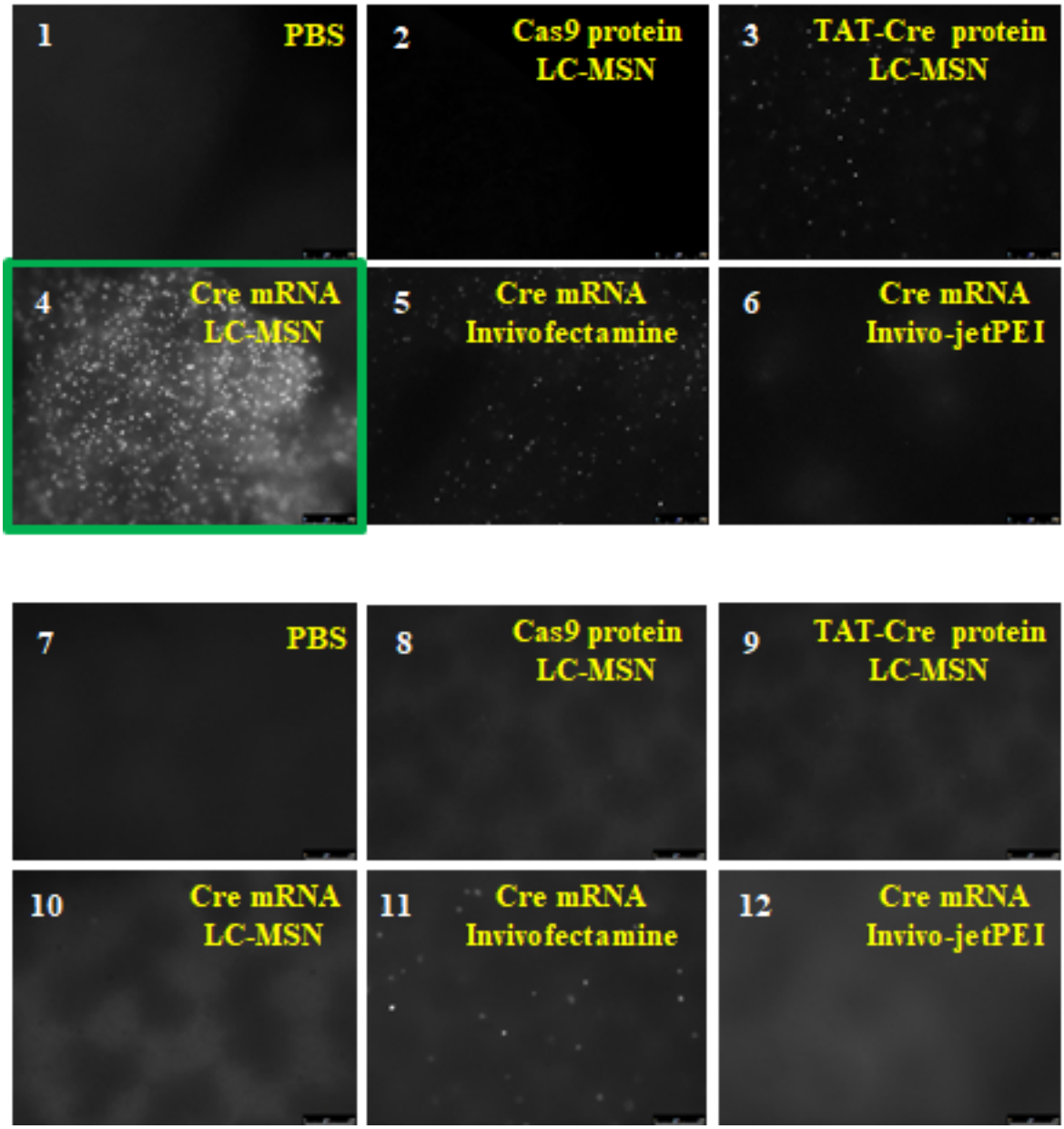

Figure 1. Preliminary Evidence Suggesting that LC-MSNs Can Effectively Deliver mRNA to Lung. LC-MSNs (100 μg) loaded with Cre mRNA (5 μg) were administered to Ai9 mice [7] *via* oropharyngeal aspiration (OPA) [8]. Alternative combinations of delivery vehicle and cargo (listed first and second, respectively, in each panel) were tested in parallel. Each treatment was tested in 4 animals, except for phosphate buffered saline (PBS) (negative control), which was tested in only 2 animals. At 4 days (d) post-treatment, tissues were collected from each animal and immediately analyzed for red fluorescence (indicative of Cre activity leading to tdTomato expression) *via* whole-tissue imaging *via* microscopy. Representative images from the lung (top) and liver (bottom) of one

animal *per* treatment are shown. No fluorescence above background (PBS) was detected in spleen or kidney (not shown).

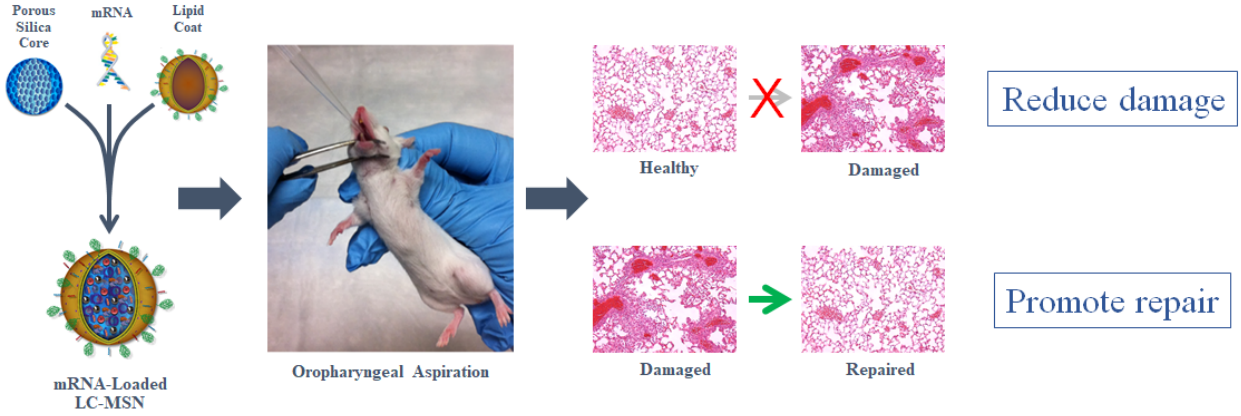

Figure 2. Overview of Project's Approach and Goal. We sought to confirm our preliminary results suggesting that LC-MSNs can mediate effective delivery of mRNA to lung when administered *via* OPA. Upon establishing proof of concept and standardized methods, we would then use this approach to evaluate candidate therapeutic mRNAs with respect to their ability to prevent and/or repair lung damage in mouse.

2. AIM 1: CONFIRM THAT NANOPARTICLES EFFECTIVELY DELIVER REPORTER-ENCODING MESSENGER RNA TO LUNG.

2.1. LC-MSN Mediated Delivery of Cre mRNA to Lung in Ai9 Mice.

Our initial results suggested that LC-MSNs mediate effective delivery of Cre mRNA to the lung when administered *via* OPA, as evident from tdTomato expression in the Ai9 mouse (**Figure 1**). However, the results were considered preliminary, because they were derived from a single study of 2-4 mice *per* cohort. Our first objective was to repeat the study in order to confirm its results. Over the course of ~6 months (mo), we carried out 5 independent studies in which LC-MSNs were used to deliver Cre mRNA to lung in Ai9 mice. These studies used 3-6 mice *per* cohort, and examined several different variables:

- MSN structure: Hexagonal (hex) (which has larger pores) *vs* stellate (which has higher surface area) configuration.
- Cre mRNA amount: 1 *vs* 2 *vs* 4 μg encapsulated mRNA, as evident from RiboGreen fluorescence.
- Lipid coat composition: DCD3330 (33:33:30:4 DOTAP:DOPE:cholesterol:PEG2000 PE (18:1) [9] *vs* variations with DOTAP at 10 *vs* 20 *vs* 50 molar fraction (mol%).
- Lipid carrier: None *vs* human apolipoprotein E3 (hApoE3) (0.15 ng/μl) *vs* human apolipoprotein E4 (hApoE4) (0.15 ng/μl).
- Expression period: Detection at 2 *vs* 6 *vs* 16 *vs* 24 *vs* 48 hours (h) post-administration.

Cre mRNA was loaded into MSNs in a solution of 750 μM triethylammonium acetate (pH 4.5), and the combination encapsulated with lipid *via* sonication in the presence of liposomes. The mRNA-loaded LC-MSNs were then washed with, and resuspended in, PBS.

Ai9 mice were anaesthetized to deep surgical plane with inhaled isoflurane (5%), then administered 30 μl of mRNA-loaded LC-MSNs in PBS *via* OPA. The mice were observed and weighed 2 times *per* day (d); the mice were found to be healthy in appearance, behavior, and weight gain in all cases except when 50% DOTAP was incorporated (see below). At pre-defined times, mice were euthanized by carbon dioxide inhalation, and their tissues of interest (lung, liver, spleen, and kidney) collected into PBS.

Measurement of red fluorescence (due to mRNA-mediated production of Cre recombinase, resulting in expression of TdTomato) in the tissues was accomplished using an *in vivo* imaging system (IVIS), a vast improvement over the microscopy-based detection used in our initial study, which was not quantitative. For IVIS, the tissues were removed from PBS, arranged upon a black backdrop, and then analyzed using a 520 nm excitation filter and a 580, 600, 620, or 640 nm emission filter (results were similar in each case), with an exposure time of 1-10 seconds (sec).

Results from a representative experiment are shown in **Figure 3**. In this example, LC-MSNs comprised of hex *vs* stellate MSNs, plus our standard DCD3330 lipid coat, were used to encapsulate 4 μg of Cre mRNA, the LC-MSN/mRNA administered to Ai9 mice (3 *per* formulation type, plus 2 administered only PBS as a negative control) *via* OPA, and tissues collected at 1 d post-treatment for IVIS analysis (1 sec exposure, 620 nm emission). We found that administration of either LC-MSN/mRNA formulation caused an increase in red fluorescence in lung [but not liver, spleen, or kidney (not shown] due to increased expression of TdTomato, as expected. However, the

fluorescence levels were not significantly higher than those in lungs from mice administered only PBS [LC-MSN (hex) *vs* PBS *p*-value = 0.1422; and LC-MSN (stellate) *vs* PBS *p*-value = 0.1873, by unpaired Student's *t* test]. The main problem was the high background of red fluorescence (*i.e.*, autofluorescence in red spectrum) in lung, regardless of treatment condition. This problem was not resolved to satisfaction through use of background subtraction software. Up to 20% DOTAP (previously shown to improve lung targeting of systemically-administered LNPs [10]) was well tolerated but didn't improve mRNA delivery; whereas LC-MSN/mRNA formulations with 50% DOTAP caused breathing issues and damage to lung tissue (not shown). In the final analysis, the results from this series of studies were consistent with the idea that LC-MSNs can effectively deliver Cre mRNA to lung in the Ai9 mouse, but they did not constitute unassailable evidence supporting this conclusion.

2.2. LC-MSN Mediated Delivery of fLuc mRNA to Lung in C57Bl/6J Mice.

In order to circumvent the problem of red autofluorescence in the lung tissue of Ai9 mice, we decided to switch to a different reporter system altogether. We settled on luciferase as our reporter, primarily because its output (luminescence) is wholly absent from untreated mouse tissues (they don't produce light of any sort without expression of luciferase as well as provision of its substrate, d-luciferin). This makes for essentially no background signal whatsoever, against which any treatment-associated luminescence can be detected at high sensitivity. The other major advantage of this approach is that it doesn't require use of a specialized mouse strain like Ai9; this keeps costs low and, importantly, greatly simplifies acquisition of age-matched cohorts of mice (a formidible challenge with Ai9, often causing delays in study execution).

Over the course of ~4 mo, we carried out 6 independent studies in which LC-MSNs were used to deliver firefly luciferase (fLuc) mRNA to lung in C57Bl/6J mice. These studies used 3-6 mice *per* cohort, and examined several different variables:

- MSN structure: Hex *vs* stellate configuration.
- fLuc mRNA amount: 1 *vs* 2 *vs* 4 μg encapsulated mRNA.
- Lipid coat composition: DCD3330 *vs* variations with DOTAP at 10 *vs* 20 mol%.
- Lipid carrier: None *vs* hApoE3 (0.15 ng/μl) *vs* hApoE4 (0.15 ng/μl).
- Expression period: Detection at 2 *vs* 6 *vs* 16 *vs* 24 h post-administration.

fLuc mRNA was loaded into MSNs in a solution of 750 μM triethylammonium acetate (pH 4.5), and the combination encapsulated with lipid *via* sonication in the presence of liposomes. The mRNA-loaded LC-MSNs were then washed with, and resuspended in, PBS. LC-MSN/mRNA formulations were administered to mice *via* OPA, as described in Section 2.1. At pre-defined times, 150 μl of 20 mg/ml d-luciferin in PBS (150 mg/kg dose) were administered to each mouse *via* intraperitoneal (IP) injection, and 5 minutes (min) later tissues were collected as described in Section 2.1. For IVIS, the tissues were arranged upon a black backdrop, and then analyzed using a 565 nm emission filter, with an exposure time of 30-240 sec.

Results from a representative experiment are shown in **Figure 4**. In this example, LC-MSNs comprised of stellate MSNs and DCD3330 lipid coat were used to encapsulate 4 μg of fLuc mRNA. In some cases, a lipid carrier (hApoE3 or hApoE4) was added as well, with the idea that this could promote cell uptake [11]. Each LC-MSN/mRNA ± hApoE3/4 formulation was administered to 3 C57Bl/6J mice (and PBS was administered to 3 mice, as a negative control) *via* OPA. After 6 h, d-

luciferin was administered *via* IP injection, and tissues were collected 5 min later for IVIS analysis (30 sec exposure). We found that LC-MSN/mRNA administration was usually associated with detectable levels of luminescence (due to fLuc expression) in the lung (but not the liver, kidney, or spleen), as expected. LC-MSNs comprised of hex *vs* stellate MSNs behaved similarly, and DOTAP levels up to 20% were well tolerated but didn't improve mRNA delivery (not shown). Addition of a lipid carrier (hApoE3 or hApoE4) had no discernable positive effect (in fact, in this particular experiment inclusion of hApoE4 appeared to have a modest detrimental effect; however, this was not consistently observed throughout the series of experiments). Note that in this representative study, one of the three mice from each cohort showed no detectable luminescence in the lung [the limit of detection (LOD), 1000 arbitrary units (AU) of total luminescence intensity, is marked by the X-axis] (**Figure 4B**). The other studies in this series showed similar rates of non-detection, irrespective of the LC-MSN/mRNA formulations tested. It is not clear why this was the case. One potential cause is inconsistent administration *via* OPA, which is a simple yet tricky procedure that requires high precision and dexterity. Some personnel responsible for carrying out OPA were learning on the job, and this lack of mastery could have contributed to variability within and between studies. However, it is also possible that LC-MSN mediated delivery of mRNA is inherently inconsistent (*e.g.*, due to stochastic effects in NP uptake by cells and/or release of mRNA into the cytoplasm). *In vitro* experiments, in which LC-MSN/mRNA formulations were added to human airway epithelial (A549) cells in Petri dishes, showed greater consistency in mRNA delivery, but *in vivo* many additional barriers may come into play. In any case, the results from these experiments support the idea that LC-MSNs can effectively deliver fLuc mRNA to lung in the C57Bl/6J mouse, but inconsistency in delivery was problematic.

2.3. Lipid Nanoparticle (LNP) Mediated Delivery of fLuc mRNA to Lung in C57Bl/6J Mice.

In the context of another SNL project (Safe Genes, sponsored by DARPA), colleagues reported success with lipid nanoparticle (LNP) mediated delivery of reporter mRNA to liver *via* intravenous (IV) injection of C57Bl/6J mice. LNPs are comprised of four core components (an ionizable cationic lipid or lipidoid, a phospholipid, a PEGylated lipid, and cholesterol) that together self-assemble around a nucleic acid cargo [12]. LNP mediated delivery of mRNA *in vivo*, including to lung, had been previously demonstrated, though only through systemic administration (typically IV injection) rather than direct administration to the airway (*via* OPA, nebulization, intratracheal instillation, *etc.*) [10].

Over the course of ~4 mo, we carried out 5 independent studies in which LNPs were used to deliver fLuc mRNA to lung in C57Bl/6J mice. These studies used 5-6 mice *per* cohort, and examined several different variables:

- Ionizable cationic lipidoid: C12-200 *vs* CKK-E12.
- LNP composition: Standard [35:16:46.5:2.5 C12-200/CKK-E12:DOPE: cholesterol:PEG2000-PE (14:0)] *vs* variations with DOTAP replacing C12-200/CKK-E12, DOPE, or cholesterol at 10 *vs* 20 mol%.
- fLuc mRNA amount: 0.5 *vs* 2 *vs* 4 μg encapsulated mRNA.
- Lipid carrier: None *vs* hApoE3 (0.15 ng/μl) *vs* hApoE4 (0.15 ng/μl).
- Expression period: Detection at 6 *vs* 24 h post-administration.

The lipids were individually dissolved in 100% ethanol, then mixed in their prescribed mole ratios. fLuc mRNA was diluted in 50 mM sodium citrate (pH 4) to a concentration of 133 μg/ml, then

combined with the lipid mixture using a NanoAssemblr (total flow rate = 12 ml/min; flow rate ratio = 3:1 aqueous:organic). The mRNA-loaded LNPs were then washed with, and resuspended in, PBS. LNP/mRNA formulations were administered to mice *via* OPA as described in Section 2.1. At pre-defined times, d-luciferin was administered *via* IP injection as described in Section 2.2; and 5 min later tissues were collected as described in Section 2.1. For IVIS, the tissues were arranged upon a black backdrop, and then analyzed using a 565 nm emission filter, with an exposure time of 30-240 sec.

Results from a representative experiment are shown in **Figure 5**. In this example, LNPs of standard composition were used to encapsulate 4 µg of fLuc mRNA. In some cases, a lipid carrier (hApoE3 or hApoE4) was added as well. Each LNP/mRNA ± hApoE3/4 formulation was administered to 5 C57Bl/6J mice (PBS was administered to 5 mice, as a negative control) *via* OPA. After 6 h, d-luciferin was administered *via* IP injection, and tissues were collected 5 min later for IVIS analysis (30 sec exposure). The results from Figure 4B are included as well, for comparison. We found that LNPs effectively deliver fLuc mRNA to lung, generally supporting higher levels of luminescence (*i.e.*, expression of luciferase) as compared to LC-MSNs. DOTAP levels up to 20% were well tolerated but didn't improve mRNA delivery (not shown). Addition of a lipid carrier (hApoE3 or hApoE4) had no reproducible positive or negative effect; in this particular experiment, inclusion of hApoE3 appeared to be detrimental, and that of hApoE4 appeared to be beneficial (aside from one incidence of non-detection), but neither trend was consistently observed throughout the series of experiments.

Combining the data from the 5 experiments in this series, we found that LNPs of standard formulation, with no addition of lipid carrier, encapsulating 2-4 µg of fLuc mRNA (0.5 µg was not sufficient for effective delivery), mediated robust and consistent production of luminescence (*i.e.*, expression of luciferase) in the lung by 6 h (signals were generally weaker at 24 h), at levels averaging 629,785 AU (median = 609,822 AU) with a standard deviation of 365,619 AU) and only 2 non-detection events in a total of 31 mice (6.5% rate). In our view, these results constitute compelling proof that LNPs can effectively deliver fLuc mRNA to lung in the C57Bl/6J mouse.

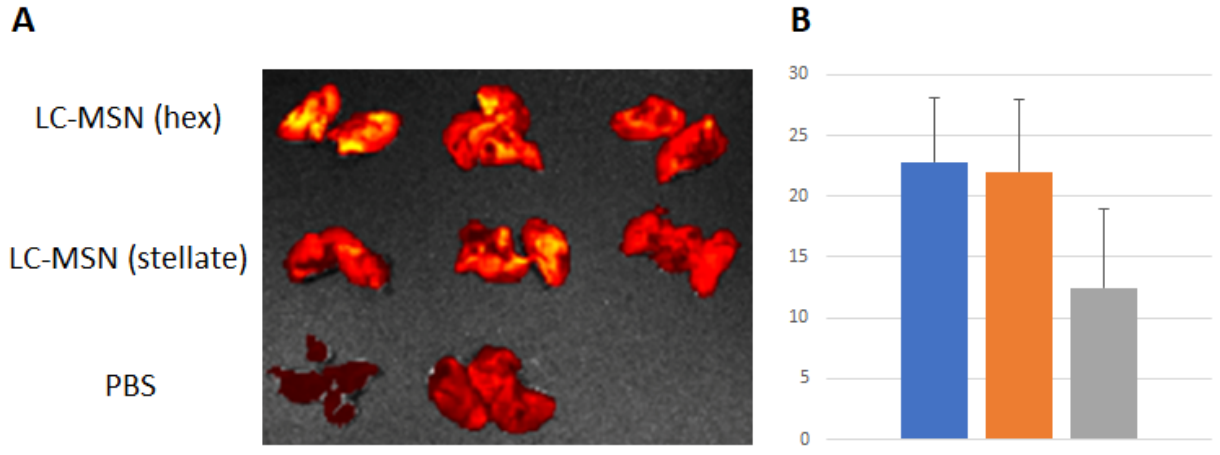

Figure 3. LC-MSN Mediated Delivery of Cre mRNA to Lung in Ai9 Mouse. LC-MSNs (100 µg) loaded with Cre mRNA (5 µg) were administered to Ai9 mice *via* OPA (3 mice *per* formulation); PBS only was administered as a negative control (2 mice). At 24 h post-treatment, tissues were collected from each animal and immediately analyzed for red fluorescence (indicative of Cre activity leading to tdTomato expression) *via* IVIS analysis (520 nm excitation, 620 nm emission). **A.** Images

of red fluorescence in lungs from mice administered LC-MSN/mRNA formulations using hex *vs* stellate MSNs. **B.** Red fluorescence intensity (arbitrary units; Y-axis) average (bar) and standard deviation (error bar) for LC-MSN (hex) *vs* LC-MSN (stellate) *vs* PBS (blue, orange, and gray bars, respectively).

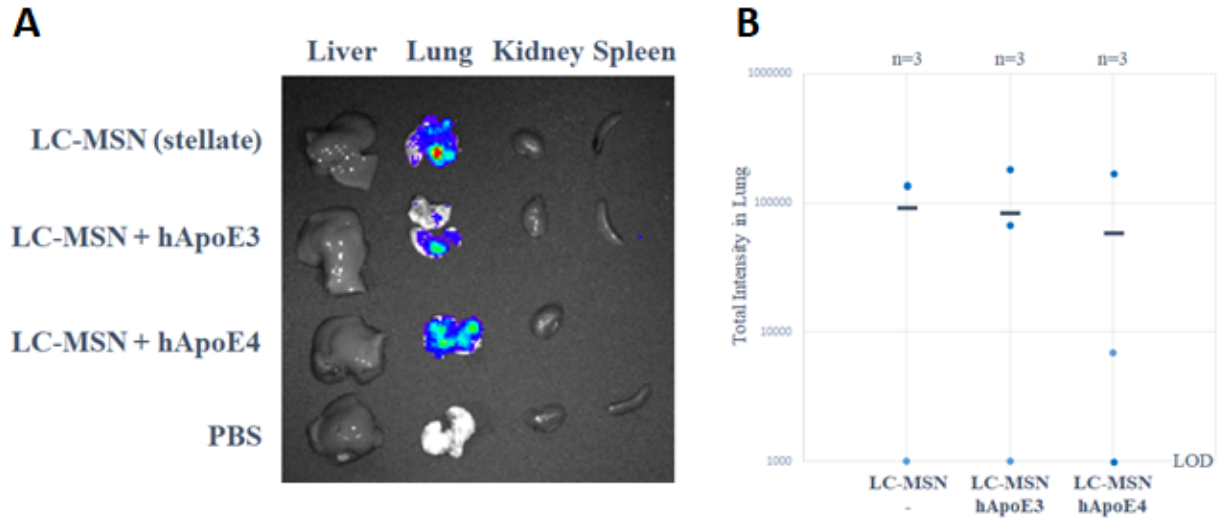

Figure 4. LC-MSN Mediated Delivery of fLuc mRNA to Lung in C57Bl/6J Mouse. LC-MSNs (100 μg) loaded with fLuc mRNA (5 μg) were administered to C57Bl/6J mice *via* OPA (3 mice *per* formulation); PBS was administered as a negative control (3 mice). At 6 h post-treatment, d-luciferin (150 μl of 20 mg/ml in PBS) was administered *via* IP injection, and 5 min later tissues were collected for immediate measurement of luminescence (indicative of luciferase expression) *via* IVIS analysis (565 nm emission). **A.** Images of luminescence in lung (but not liver, kidney, or spleen) from mice administered LC-MSN(stellate)/mRNA formulations with or without lipid carrier (hApoE3 or hApoE4). **B.** Luminescence intensity (AU; Y-axis) measurements (blue data points) and averages (black bars) are shown; LOD = 1000 AU.

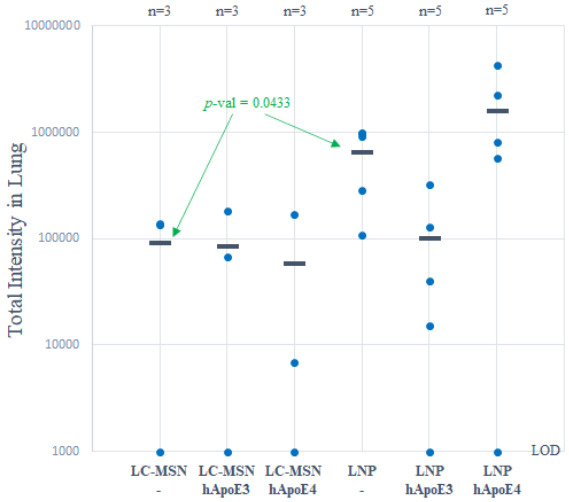

Figure 5. LC-MSN and LNP Mediated Delivery of fLuc mRNA to Lung in C57Bl/6J Mouse. LC-MSNs (100 μg) or LNPs (100 μg) loaded with fLuc mRNA (5 μg) were administered to C57Bl/6J mice *via* OPA (3-5 mice *per* formulation, as indicated at the top of the graph); PBS was administered as a negative control (8 mice in total). At 6 h post-treatment, d-luciferin (150 μl of 20 mg/ml in PBS) was administered *via* IP injection, and 5 min later tissues were collected for immediate measurement of luminescence (indicative of luciferase expression) *via* IVIS analysis (565 nm emission). Luminescence intensity (AU; Y-axis) measurements (blue data points) and averages (black bars) are shown; LOD = 1000 AU. Highlighted in green is the difference in luminescence intensity average when fLuc mRNA is delivered by LC-MSNs *vs* LNPs (*p*-value = 0.0433, by unpaired Student's *t* test).

3. AIM 2: DETERMINE WHETHER NANOPARTICLES CAN EFFECTIVELY DELIVER CANDIDATE THERAPEUTIC MESSENGER RNA TO LUNG.

3.1. Prioritization of Therapeutic mRNA Candidates.

To establish proof of concept, we sought to synthesize and evaluate mRNA equivalents of recombinant proteins that have displayed therapeutic activity in the lung in pre-clinical (animal model) and/or clinical (human) studies. Accordingly, we carried out a series of extensive searches of the scientific and medical research literatures, and of reports released by pharmaceutical and biotechnology companies as well as the Food and Drug Administration (FDA) reports, in order to identify recombinant proteins of therapeutic value in the lung. Prioritization criteria included:

- Strong evidence of therapeutic benefit, especially when administered to the airway (as opposed to administered systemically *via* IV injection, for instance).
- Extracellular site of function, such that uptake by host cells is not required for therapeutic activity (uptake may sequester the recombinant protein in a cell compartment that is not accessible to an equivalent protein produced by mRNA-instructed host cells).
- Publically available DNA (or, better yet, mRNA) sequence encoding the recombinant protein.
- Commercially available recombinant protein (for use as a positive control), especially the mouse version (as opposed to the human version, which is typically more readily available).
- Commercially available antibodies (Abs) against the recombinant protein, especially those showing reactivity to the mouse version (as opposed to those showing reactivity to the human version, which are typically more readily available).

The results from this survey are summarized in the first 10 columns of **Table 1**. The top 10 candidates are listed in order of priority (column 1). These recombinant proteins have been shown to perform a variety of functions in the lung, ranging from reduction of inflammation and coagulation, to promoting vascular barrier integrity and tissue repair (column 2). Six of the recombinant proteins have been evaluated in clinical trials; one (IL-1RA) is FDA approved, but for a different disease indication (rheumatoid arthritis) (column 4).

3.2. Synthesis and Initial Evaluation of Therapeutic mRNA Candidates.

To this point in the project, we had purchased reporter mRNA (*e.g.*, encoding fLuc) from TriLink. However, purchase of multiple custom-made mRNA would not have been cost effective, so we developed an in-house capability for synthesizing mRNA of interest. We initially focused on synthesis of fLuc mRNA, which could be assessed with regard to function using methods already established (Aim 1). After directly testing several different approaches, we settled on use of a commercially available kit for T7 promoter based *in vitro* transcription (IVT): HiScribe T7 High Yield RNA Synthesis Kit (New England BioLabs). DNA templates for IVT were constructed *via* Gibson assembly of purchased gBlocks (IDT). For 5' capping of mRNA, we used CleanCap Reagent AG (TriLink) at a 1:1 ratio with guanine-5'-triphosphate. For 3' tailing of mRNA, we tested 40 *vs* 60 poly-adenylation, and found that the latter supported slightly better expression both *in vitro* and *in vivo*. Finally, we substituted a modified ribonucleotide (N1-methylpseudouridine) for uridine-5'-triphosphate, to improve mRNA stability and translation, and reduce intracellular innate immunogenicity [13,14].

After verifying that fLuc mRNA synthesized through our IVT approach effectively mediates fLuc production *in vitro* and *in vivo*, we similarly synthesized mRNA encoding our therapeutic recombinant proteins of interest. These mRNA were introduced into host cells [airway epithelial cell lines A549 (human) and LA-4 (mouse)] using a transfection reagent (Lipofectamine MessengerMax), and their ability to mediate expression of the therapeutic protein assessed *via* Western analysis of cell lysates. In some cases, detection of the expressed protein was straightforward; an example is shown in **Figure 6A**. In others, however, detection was apparently confounded by two different effects: 1) Masking of the recombinant protein by expression of the endogenous version of the protein; and 2) Poor specificity of the Abs used for detection. Accordingly, we constructed a second set of IVT templates for synthesis of mRNA encoding each therapeutic protein fused to a standard epitope tag (FLAG; sequence = DDDDK) *via* a short linker sequence (GGSGGDYK). These FLAG-tagged proteins were readily detected *in vitro* using a highly-specific monoclonal anti-FLAG Ab conjugated to horse radish peroxidase (HRP) (Abcam ab49763), which generates a luminescence signal (**Figure 6B**). A summary of the results from the A549 transfection experiments can be found in **Table 1** (column 12).

mRNA encoding the untagged and FLAG-tagged proteins were then encapsulated into LNPs, and these administered to mice *via* OPA, using the methods described in Section 2.3; and expression of the therapeutic proteins detected in lung homogenates *via* Western analysis. We found that detection of the FLAG-tagged proteins was generally robust and unambiguous, with the exception of IL-22-FLAG, which apparently was not expressed well in lung. Untagged versions of 3 of the proteins (rhTM, sACE2-IgG, GM-CSF) were also detected robustly and unambiguously, whereas a fourth (TFPI) showed little to no expression in lung. Results from a representative experiment are shown in **Figure 7**. A summary of the results from the full series of lung delivery experiments can be found in **Table 1** (column 13).

3.3. Establishment of a Mouse Model of Severe Lung Damage.

The final step in evaluating our mRNA equivalents of therapeutic recombinant proteins was to determine whether they could provide protection against lung damage in mice. To this end, we sought to establish a mouse model of severe lung damage, ideally one in which the disease is acutely lethal, as this would offer opportunity to measure protective activity *via* survival analysis (*i.e.*, assessment as to whether an LNP/mRNA formulation could reduce mortality and "rescue" mice), a simple and well-accepted approach. Additionally, use of a non-infectious causative agent was desirable, given that our candidate mRNA-based therapies are designed to promote lung resiliency and tissue repair, rather than to counter infection. Acute respiratory distress syndrome (ARDS) models are commonly based on inhalational challenge with bacterial lipopolysaccharide (LPS), which triggers many of the same cellular and immune responses as infection, leading to acute lung injury and respiratory failure. However, the disease is relatively mild in mouse, typically resolving within 2-3 d without intervention [15,16]. In contrast, ARDS resulting from infection is often lethal in humans, and characterized by profound dysregulation of immune responses, which causes extensive tissue and vascular damage, hypercoagulation, and cytokine release syndrome, necessitating intensive care in a hospital setting. Through an extensive survey of the literature, we identified an elaboration of the LPS challenge method that is reported to more faithfully recapitulate the hallmark features of human ARDS. In this approach, pre-treatment with α-galactosylceremide (αGalCer), an immune stimulant that activates natural killer T (NKT) cells, potentiates and magnifies the innate immune responses provoked by LPS challenge, thereby causing severe and often lethal ARDS-like disease [17,18]. We hypothesized that this model system would support sensitive detection of therapeutic effects resulting from treatment with our mRNA equivalents of therapeutic recombinant proteins.

We carried out a series of 4 independent studies to develop an αGalCer + LPS dosing regimen that reproducibly results in acute lung damage and high mortality in C57Bl/6J mice. These studies used 3-6 mice *per* cohort, and examined several different variables:

- αGalCer dose: 2 *vs* 3 *vs* 5 μg.
- LPS dose: 25 *vs* 75 *vs* 150 μg.
- Potentiation period: 1 *vs* 2 d.

Results from a representative experiment are shown in **Figure 8**. In this experiment and others, we found that an αGalCer dose of 5 μg, in combination with an LPS dose of 75-150 μg, is sufficient to cause significant mortality in C57Bl/8J mice. The impact of potentiation period on mortality was not consistent within and between experiments; for instance, in the experiment shown in **Figure 8**, a shorter potentiation period (1 d) was associated with higher mortality when dosing with 5 μg αGalCer + 75 μg LPS, but lower mortality when dosing with 5 μg αGalCer + 150 μg LPS. Weighing all of the evidence, we decided to go forward with 5 μg αGalCer + 150 μg LPS (2 d potentiation period) as our standard dosing regimen.

Protein	Therapeutic Function	Drug	Regulatory Status	mRNA Length (nt)	Site of Protein Function	Reference (DOI)	Recombinant Protein (Mouse)	Recombinant Protein (Human)	Antibodies	IVT Template	Expression in A549	Expression in Lung	Impact on Survival
IL-1RA	Reduces inflammation	Anakinra (Kineret)	FDA approved (RA)	1671	Extracellular	10.1097/CCM.0000000000001402 10.1016/S2665-9913(20)30127-2 10.1016/S2665-9913(20)30160-0	Sigma SRP6006	Sigma SRP3327	Abcam ab124962: Rabbit mAb (M, H)	**Untagged:** Success **FLAG-tagged:** Success	**Untagged:** not clear **FLAG-tagged:** Success	Untagged: not done **FLAG-tagged:** Success	Untagged: not done **FLAG-tagged:** not clear
rhTM	Reduces coagulation & inflammation	ART-123 (Recomodulin)	Phase III (ARDS, sepsis)	4040	Extracellular	10.2147/DDDT.S68030 10.1186/s13054-019-2521-7	Elabscience PKSM041274	PeproTech 100-58	Abcam ab109189: Rabbit mAb (H)	**Untagged:** Success **FLAG-tagged:** Success	**Untagged:** Success **FLAG-tagged:** Success	**Untagged:** Success **FLAG-tagged:** Success	Untagged: not done **FLAG-tagged:** not clear
sACE2-IgG	Promotes vascular barrier integrity (also a decoy receptor for SARS-CoV-2)	rhACE2	Phase II (ARDS)	3339	Extracellular	10.12688/f1000research.22211.2	Elabscience PKSM040780 Boster PROTQ8R010	Boster RCOV09 Boster RCOV10	protein A	**Untagged:** Success **FLAG-tagged:** Success	**Untagged:** Success **FLAG-tagged:** Success	**Untagged:** Success **FLAG-tagged:** Success	Untagged: not done **FLAG-tagged:** not clear
TFPI	Reduces coagulation & inflammation	Tifacogin	Phase II (sCAP, sepsis)	1179	Extracellular	10.1089/jamp.2016.1317 10.1159/000453002	R&D Systems 2975-PI Elabscience PKSM040845	R&D Systems 2974-PI Boster PROTP10646 Sigma SRP6458	Abcam ab180619: Rabbit pAb (M, H)	**Untagged:** Success **FLAG-tagged:** Success	**Untagged:** Success **FLAG-tagged:** Success	**Untagged:** not clear **FLAG-tagged:** Success	Untagged: not done **FLAG-tagged:** not clear
IL-22	Reduces inflammation, promotes tissue repair	UTTR1147A	Phase II (UC)	1165	Extracellular	10.1038/mi.2012.49 10.1038/s41598-017-11518-0 10.1136/thoraxjnl-2017-211097 10.1038/s41385-019-0206-9	enQuire QP10463 Boster PROTQ9JJY9-3	Elabscience PKSH032632	Abcam ab18564: Rabbit pAb (M)	**Untagged:** Success **FLAG-tagged:** Success	**Untagged:** not clear **FLAG-tagged:** Success	Untagged: not done **FLAG-tagged:** not clear	Untagged: not done FLAG-tagged: not done
GM-CSF	Promotes tissue repair	Molgramostim	Phase II (PAP)	788	Extracellular	10.1097/CCM.0b013e31822d7bf0 10.1164/rccm.201311-2041LE	Elabscience PKSM041031	Elabscience PKSH032504	Abcam ab227031: Rabbit mAb (M, H), no WB Abcam ab9741: Rabbit pAb (H) Abcam ab271265: Rabbit pAb-biotin (M)	**Untagged:** Success **FLAG-tagged:** Success	**Untagged:** Success **FLAG-tagged:** Success	**Untagged:** Success **FLAG-tagged:** Success	Untagged: not done **FLAG-tagged:** not clear
AREG	Reduces inflammation, promotes tissue repair	-	Pre-clinical	1234	Extracellular	10.1016/j.immuni.2015.01.020 10.1126/science.1233632	Abbexa abx652492	Boster PROTP15514-1 Shenandoah 100-206	Abcam ab244674: Rabbit mAb (M), WB?	**Untagged:** Success **FLAG-tagged:** Success	**Untagged:** not clear **FLAG-tagged:** Success	Untagged: not done **FLAG-tagged:** Success	Untagged: not done **FLAG-tagged:** not clear
ANGPT1	Promotes vascular barrier integrity	-	Pre-clinical	4230	Extracellular	10.1016/j.cyto.2011.04.005 10.1101/2020.03.30.016147	R&D Systems 9936-AN Cell Sciences CRM584A-His	R&D Systems 923-AN OriGene TP723011 Abnova P5939	Abcam ab8451: Rabbit pAb (M, H)	**Untagged:** Success **FLAG-tagged:** Success	**Untagged:** not clear **FLAG-tagged:** Success	Untagged: not done **FLAG-tagged:** Success	Untagged: not done **FLAG-tagged:** not clear
HMOX1	Reduces inflammation-associated oxidative stress	-	Pre-clinical	1554	Extracellular	10.1155/2016/4158698 10.1165/rcmb.2006-0311OC 10.4049/jimmunol.1601414	-	Elabscience PKSH032529 Boster PROTP09601 Abbexa abx073058	Abcam ab52947: Rabbit mAb (M, H)	**Untagged:** Success **FLAG-tagged:** Success	**Untagged:** not clear **FLAG-tagged:** Success	Untagged: not done **FLAG-tagged:** Success	Untagged: not done **FLAG-tagged:** not clear
TRIM72	Promotes tissue repair	-	Pre-clinical	8402	ER	10.1165/rcmb.2017-0364OC	-	-	Abcam ab238252: Goat pAb-biotin (M, H)	**Untagged:** Success **FLAG-tagged:** Success	**Untagged:** not clear **FLAG-tagged:** not clear	Untagged: not done FLAG-tagged: not done	Untagged: not done FLAG-tagged: not done

Table 1. Therapeutic Recombinant Proteins of Interest, and Summary of Results from Synthesis and Testing of mRNA Equivalents.

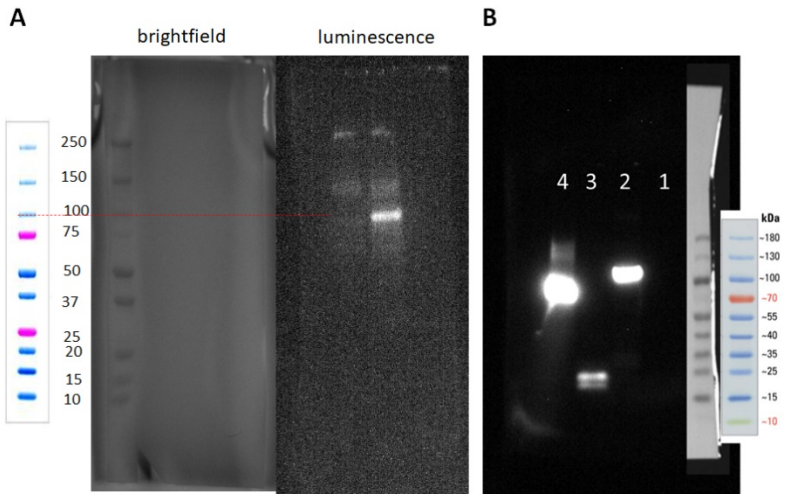

Figure 6. Western Analysis of mRNA-Instructed Expression of Therapeutic Recombinant Proteins *In Vitro*. A. mRNA-instructed expression of sACE2-IgG in A549 cells. 15 µg of sACE2-IgG mRNA were combined with 30 µl of transfection reagent (Lipofectamine MessengerMax), and the mixture added to ~$6x10^6$ cells. After incubation for 16 h at 37°C, the cells were collected into 400 µl lysis buffer containing 2% SDS and protease inhibitors, sonicated in a water bath for 1 hr at 37°C, and the lysate (31.25 µg total protein) subjected to SDS-PAGE (4-15% gel) followed by transfer to a PVDF membrane and detection using an HRP-conjugated monoclonal goat anti-mouse Ab against ACE2. The brightfield image (left) shows the positions of molecular weight markers for reference; the luminescence image (right) shows Ab-mediated detection of sACE2-IgG (expected size = 93 kDa) in transfected cells (second lane) but not in naive cells (first lane). **B.** mRNA-instructed expression of sACE2-IgG-FLAG in A549 cells. mRNA encoding FLAG-tagged versions of three therapeutic proteins of interest were introduced into cells, and proteins translated from them detected *via* Western analysis, using the methods described above in combination with an HRP-conjugated monoclonal mouse Ab against FLAG. First lane: naive cells; second lane: cells expressing sACE2-IgG-FLAG (expected size = 98 kDA); third lane: cells expressing GM-CSF-FLAG (expected size = 17 kDA); fourth lane: cells expressing rhTM-FLAG (expected size = 56 kDA).

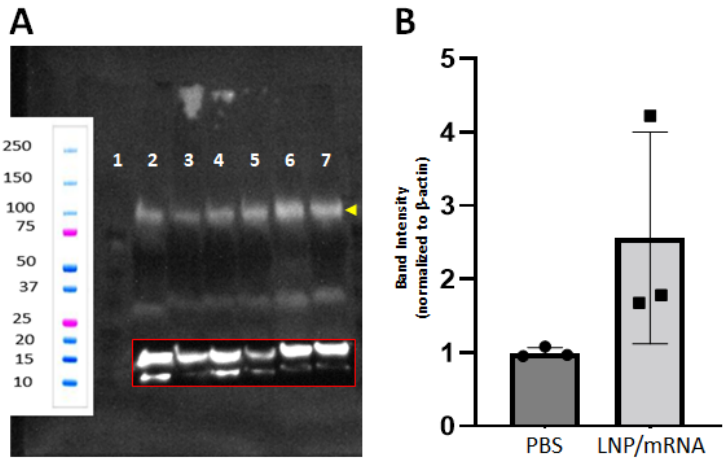

Figure 7. Western Analysis of mRNA-Instructed Expression of a Therapeutic Recombinant Protein *In Vivo*. 2 μg of sACE2-IgG mRNA was encapsulated in LNPs, and the formulation administered to 3 mice *via* OPA. PBS was administered to another 3 mice, to serve as a negative control. All animals were euthanized at 6 h post-treatment, and their lungs were collected and homogenized. The homogenates (each 300 μg total protein) were subjected to SDS-PAGE (4-15% gel) followed by transfer to a PVDF membrane. Expression of sACE2-IgG was detected using an HRP-conjugated monoclonal mouse anti-mouse Ab against ACE2. Then, the membrane was stripped, and β-actin (an abundant housekeeping protein, here serving as a protein loading marker) was detected using an HRP-conjugated monoclonal goat anti-mouse Ab against β-actin. **A.** Image of Western blot luminescence. Lane 1: Molecular weight marker; lanes 2-4: PBS treatment; lanes 5-7: sACE2-IgG mRNA treatment. Yellow arrowhead indicates expected size of sACE2-IgG (93 kDa). Red box indicates luminescence associated with β-actin detection (superimposed upon the image of sACE2-IgG detection, for comparison). **B.** Graph of sACE2-IgG band intensities normalized by β-

actin band intensities (loading control). Bars indicate average normalized band intensity; error bars indicate standard deviation.

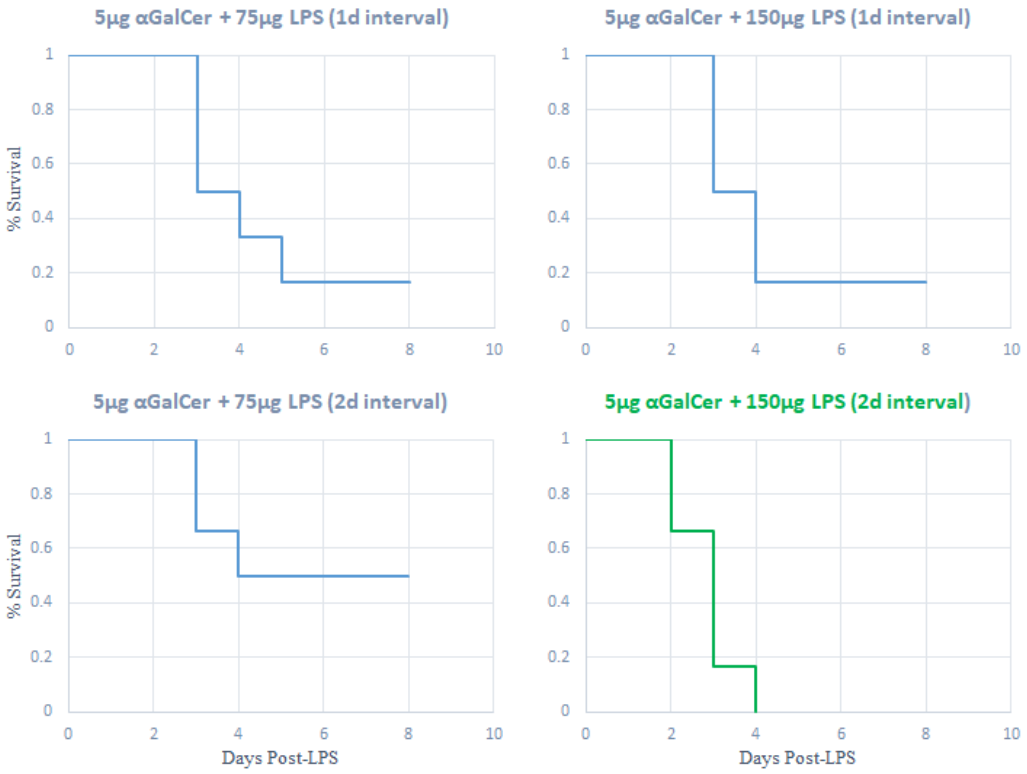

Figure 8. Mortality as a Function of αGalCer + LPS Dosing Regimen. αGalCer (5 μg) and LPS (75-150 μg) were sequentially (1-2 d interval) administered to C57Bl/6J mice (6 *per* treatment condition) *via* OPA, and mortality monitored for 8 d following LPS treatment.

3.4. Evaluation of Therapeutic mRNA Candidates in Treating Severe Lung Damage.

The 8 mRNA that mediate detectable expression of FLAG-tagged therapeutic proteins in lung (**Table 1**, column 13) were evaluated for ability to reduce mortality in our newly established mouse model of severe lung damage. In this experiment, the 5 μg αGalCer + 150 μg LPS (2 d potentiation period) dosing regimen was applied, and then 1 d later the LNP/mRNA formulations were administered to the mice using the methods described in Section 2.3. We included two negative controls as well: 1) Administration of PBS alone; and 2) Administration of LNP/fLuc mRNA, which was not expected to show a therapeutic effect. Each treatment was applied to 8 mice, and mortality was monitored for 10 d. The results of this experiment are shown in **Figure 9**.

We were surprised to find that our standard αGalCer + LPS dosing regimen was less lethal in this experiment than in previous ones (see Section 3.3), such that the PBS-treated cohort showed 25% survival (rather than 0%). This was fortuitous in a way, however, because it served as a sensitive

background against which we were able to detect an unexpected increase in mortality upon treatment with LNP/fLuc mRNA (0% survival). To this point in the project, we had seen no signs of toxicity associated with LNP/fLuc mRNA, but importantly, we had administered it only to healthy mice. The results from this experiment indicate that administration of LNP/fLuc mRNA (and potentially other LNP/mRNA formulations) to mice with severe lung damage may contribute to mortality.

Using the LNP/fLuc mRNA treatment condition as a baseline (to account for toxicity assocated with LNP/mRNA administration), we found that several of the other LNP/mRNA treatments [IL-1RA(FLAG), sACE2-IgG(FLAG), and ANGPT1(FLAG)] reduced mortality to a modest degree (to 25% survival, rather than 0% survival), though these therapeutic effects did not reach statistical significance (**Figure 9** and **Table 2**). The remaining LNP/mRNA treatments showed even weaker therapeutic effects, with the exception of LNP/GM-CSF(FLAG) mRNA treatment, which showed no therapeutic effect (and perhaps additional toxicity, as indicated by a Mantel-Haenszel Hazard Ratio of <1). These results suggest that the IL-1RA(FLAG), sACE2-IgG(FLAG), and ANGPT1(FLAG) LNP/mRNA formulations should be prioritized for further assessment of therapeutic effects.

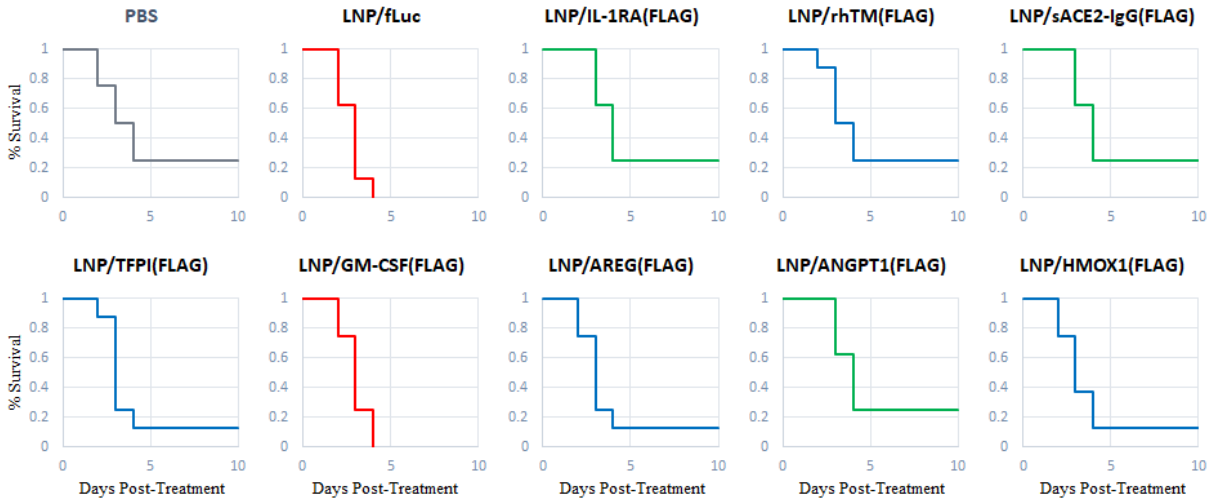

Figure 9. Assessment of Candidate Therapeutic mRNA for Ability to Reduce Mortality in a Mouse Model of Severe Lung Damage. αGalCer (5 μg) and LPS (150 μg) were sequentially (2 d interval) administered to C57Bl/6J mice *via* OPA in order to induce lung damage. At 1 d post LPS administration, either PBS (negative control) or an LNP/mRNA formulation (2 μg mRNA) was

administered *via* OPA (8 mice *per* treatment condition). Mortality was monitored for 10 d following treatment.

Treatment 1	Treatment 2	Cox-Mantel Log-Rank Test *p*-value	Mantel-Haenszel Hazard Ratio
PBS	LNP/fLuc	0.115	0.319
LNP/fLuc	LNP/IL-RA(FLAG)	0.016	6.341
LNP/fLuc	LNP/rhTM(FLAG)	0.065	3.933
LNP/fLuc	LNP/sACE2-IgG(FLAG)	0.016	6.341
LNP/fLuc	LNP/TFPI(FLAG)	0.213	2.659
LNP/fLuc	LNP/GM-CSF(FLAG)	0.482	0.565
LNP/fLuc	LNP/AREG(FLAG)	0.363	1.994
LNP/fLuc	LNP/ANGPT1(FLAG)	0.016	6.341
LNP/fLuc	LNP/HMOX1(FLAG)	0.242	2.392

Table 2. Results from Statistical Comparison of Survival Curves Shown in Figure 9. Green indicates a modest reduction of mortality that did not reach statistical significance (*p*-value threshold of 0.011 when factoring in Bonferroni correction for multiple comparisons). Red indicates a Mantel-Haenszel Hazard Ratio of <1 (*i.e.*, risk of mortality associated with Treatment 2 is greater than that associated with Treatment 1).

4. CONCLUSIONS AND FUTURE DIRECTIONS.

Over the course of this project, we were able to make a number of significant technical advancements that offer a promising path forward to development of new MCMs against respiratory disorders.

4.1. Conclusions.

- LC-MSNs can effectively deliver reporter mRNA to lung.
    - Confirmed initial observation that LC-MSNs can mediate delivery of Cre mRNA to lung in the Ai9 mouse. However, tdTomato expression (due to Cre expression and activity) was low, and red fluorescence background was high, so evidence for effective delivery was weak.
    - Delivery of fLuc mRNA in the C57Bl/6J mouse was easier to measure, due to lack of luminescence background; however, signals were still weak.
    - LC-MSN variations in MSN structure, lipid coat, and lipid carrier had no marked effect on mRNA delivery.
    - No off-target expression was detected in other tissues (liver, kidney, or spleen).
    - Delivery success rate (*i.e.*, percentage of animals in which delivery-specific fluorescence/luminescence was observed) was reasonably high (~70%).
- LNPs can effectively deliver mRNA to lung with greater consistency.
    - Initially demonstrated through delivery of fLuc mRNA in the C57Bl/6J mouse. Effective delivery of mRNA equivalents of therapeutic recombinant proteins demonstrated that LNPs are capable of delivering mRNA that vary in sequence composition and length.
    - LNP variations in lipid composition and lipid carrier had no marked effect on mRNA delivery.
    - No off-target expression was detected in other tissues (liver, kidney, or spleen).
    - Delivery success rate (*i.e.*, percentage of animals in which delivery-specific luminescence was observed) was very high (~93.5%).
- LNP-mediated delivery of mRNA equivalents of therapeutic recombinant proteins is a promising strategy for treating lung damage.
    - Delivery of mRNA encoding FLAG-tagged IL-1RA, sACE2-Ig, and ANGPT1 reduced mortality to a modest degree in our newly established mouse model of severe lung damage resembling ARDS.

4.2. Future Directions.

- Optimize αGalCer + LPS dosing regimen to achieve a consistent mortality rate in our mouse model of severe lung damage. This should improve our ability to sensitively detect and precisely measure therapeutic effects associated with mRNA delivery.
    - Consider increasing αGalCer and/or LPS dose, and/or multiple rounds of dosing.
- Optimize LNP/mRNA formulation for effective delivery without toxicity when administered to mice with severe lung damage. Success will be essential for translation to clinical use.
- Further evaluate IL-RA, sACE2-Ig, and ANGPT1 mRNA as MCMs against lung damage.

    - Repeat study of therapeutic effects, using a less toxic LNP/mRNA formulation and a mouse model with a more consistent mortality rate.
    - Assess potential for prophylactic effects, by administering prior to lung damage.
    - Evaluate combination therapy/prophylaxis, by administering multiple LNP/mRNA formulations simultaneously or sequentially.
    - Test efficacy in treating/preventing lung damage resulting from other causes, such as physical stresses and infectious diseases.
    - Recapitulate most promising effects in non-human primate (NHP) model(s), as initial step in assembling a data package to support authorization of clinical trials. This will require a partner with access to a NHP research facility.
- Investigate whether LNP-mediated delivery of 8 mRNA equivalents of therapeutic recombinant proteins confers any benefit to healthy mice (*e.g.*, increased lung capacity).
    - DoD has expressed interest in treatments that enhance lung performance.

REFERENCES

[1] Sharma VK, Watts JK (2015) Oligonucleotide therapeutics: Chemistry, delivery, and clinical progress. Future Med Chem 7:2221-42. DOI: 10.4155/fmc.15.144.

[2] Weng Y, Li C, Yang T, Hu B, Zhang M, Guo S, Xiao H, Liang XJ, Huang Y (2020) The challenge and prospect of mRNA therapeutics landscape. Biotechnol Adv 40:107534. DOI: 10.1016/j.biotechadv.2020.107534.

[3] Kauffman KJ, Webber MJ, Anderson DG (2016) Materials for non-viral intracellular delivery of messenger RNA therapeutics. J Control Release 240:227-34. DOI: 10.1016/j.jconrel.2015.12.032.

[4] Chen J, Tang Y, Liu Y, Dou Y (2018) Nucleic acid based therapeutics for pulmonary diseases. AAPS PharmSciTech 19:3670-80. DOI: 10.1208/s12249-018-1183-0.

[5] Kowalski PS, Rudra A, Miao L, Anderson DG (2019) Delivering the messenger: Advances in technologies for therapeutic mRNA delivery. Mol Ther 27:710-28. DOI: 10.1016/j.ymthe.2019.02.012.

[6] Butler KS, Durfee PN, Theron C, Ashley CE, Carnes EC, Brinker CJ (2016) Protocells: Modular mesoporous silica nanoparticle supported lipid bilayers for drug delivery. Small 12:2173-85. DOI: 10.1002/smll.201502119.

[7] Madisen L, Zwingman TA, Sunkin SM, Oh SW, Zariwala HA, Gu H, Ng LL, Palmiter RD, Hawrylycz MJ, Jones AR, Lein ES, Zeng H (2010) A robust and high-throughput Cre reporting and characterization system for the whole mouse brain. Nat Neurosci 13:133-40. DOI: 10.1038/nn.2467.

[8] Schully KL, Bell MG, Ward JM, Keane-Myers AM (2014) Oropharyngeal aspiration of *Burkholderia mallei* and *Burkholderia pseudomallei* in BALB/c mice. PLoS ONE 9:e115066. DOI: 10.1371/journal.pone.0115066.

[9] LaBauve AE, Rinker TE, Noureddine A, Serda RE, Howe JY, Sherman MB, Rasley A, Brinker CJ, Sasaki DY, Negrete OA (2018) Lipid-coated mesoporous silica nanoparticles for the delivery of the ML336 antiviral to inhibit encephalitic alphavirus infection. Sci Rep 8:13990. DOI: 10.1038/s41598-018-32033-w.

[10] Cheng Q, Wei T, Farbiak L, Johnson LT, Dillard SA, Siegwart DJ (2020) Selective organ targeting (SORT) nanoparticles for tissue-specific mRNA delivery and CRISPR-Cas gene editing. Nat Nanotechnol 15:313-20. DOI: 10.1038/s41565-020-0669-6.

[11] Dong Y, Love KT, Dorkin JR, Sirirungruang S, Zhang Y, Chen D, Bogorad RL, Yin H, Chen Y, Vegas AJ, Alabi CA, Sahay G, Olejnik KT, Wang W, Schroeder A, Lytton-Jean AKR, Siegwart DJ, Akinc A, Barnes C, Barros SA, Carioto M, Fitzgerald K, Hettinger J, Kumar V, Novobrantseva TI, Qin J, Querbes W, Koteliansky V, Langer R, Anderson DG (2014)

Lipopeptide nanoparticles for potent and selective siRNA delivery in rodents and nonhuman primates. Proc Natl Acad Sci USA 111:3955-60. DOI: 10.1073/pnas.1322937111.

[12] Eygeris Y, Gupta M, Kim J, Sahay G (2022) Chemistry of lipid nanoparticles for RNA delivery. Acc Chem Res 55:2-12. DOI: 10.1021/acs.accounts.1c00544.

[13] Andries O, McCafferty S, DeSmedt SC, Weiss R, Sanders NN, Kitada T (2015) N(1)-methylpseudouridine-incorporated mRNA outperforms pseudouridine-incorporated mRNA by providing enhanced protein expression and reduced immunogenicity in mammalian cell lines and mice. J Control Release 217:337-44. DOI: 10.1016/j.jconrel.2015.08.051.

[14] Nance KD, Meier JL (2021) Modifications in an emergency: The role of N1-methylpseudouridine in COVID-19 vaccines. ACS Cent Sci 7:748-56. DOI: 10.1021/acscentsci.1c00197.

[15] D'Alessio FR (2018) Mouse models of acute lung injury and ARDS. Methods Mol Biol 1809:341-50. DOI: 10.1007/978-1-4939-8570-8_22.

[16] Aeffner F, Bolon B, Davis IC (2015) Mouse models of acute respiratory distress syndrome: A review of analytical approaches, pathologic features, and common measurements. Toxicol Pathol 43:1074-92. DOI: 10.1177/0192623315598399.

[17] Aoyagi T, Yamamoto N, Hatta M, Tanno D, Miyazato A, Ishii K, Suzuki K, Nakayama T, Taniguchi M, Kunishima H, Hirakata Y, Kaku M, Kawakami K (2011) Activation of pulmonary invariant NKT cells leads to exacerbation of acute lung injury caused by LPS through local production of IFN-gamma and TNF-alpha by Gr-1+ monocytes. Int Immunol 23:97-108. DOI: 10.1093/intimm/dxq460.

[18] Aoyagi T, Sato Y, Toyama M, Oshima K, Kawakami K, Kaku M (2019) Etoposide and corticosteroid combination therapy improves acute respiratory distress syndrome in mice. Shock 52:83-91. DOI: 10.1097/SHK.0000000000001231.

DISTRIBUTION

Name	Org.	Sandia Email Address
Joseph Schoeniger	8623	jsschoe@sandia.gov
Technical Library	1911	sanddocs@sandia.gov

This page left blank

Sandia National Laboratories

Sandia National Laboratories is a multimission laboratory managed and operated by National Technology & Engineering Solutions of Sandia LLC, a wholly owned subsidiary of Honeywell International Inc. for the U.S. Department of Energy's National Nuclear Security Administration under contract DE-NA0003525.